

Article

Not peer-reviewed version

---

# Predicting Neighborhood-Level Residential Carbon Emission from Street-view Images Using Computer Vision and Machine Learning

---

[Wangqi Shi](#) , Yeyu Xiang , Yuxuan Ying , Yuqin Jiao , Rui Zhao , [Waishan Qiu](#) \*

Posted Date: 5 February 2024

doi: 10.20944/preprints202402.0213.v1

Keywords: Carbon Emission; Residential; Neighborhood level; Street view images; Machine learning; Beijing



Preprints.org is a free multidiscipline platform providing preprint service that is dedicated to making early versions of research outputs permanently available and citable. Preprints posted at Preprints.org appear in Web of Science, Crossref, Google Scholar, Scilit, Europe PMC.

Copyright: This is an open access article distributed under the Creative Commons Attribution License which permits unrestricted use, distribution, and reproduction in any medium, provided the original work is properly cited.

Disclaimer/Publisher's Note: The statements, opinions, and data contained in all publications are solely those of the individual author(s) and contributor(s) and not of MDPI and/or the editor(s). MDPI and/or the editor(s) disclaim responsibility for any injury to people or property resulting from any ideas, methods, instructions, or products referred to in the content.

## Article

# Predicting Neighborhood-Level Residential Carbon Emission from Street-View Images Using Computer Vision and Machine Learning

Wanqi Shi <sup>1</sup>, Yeyu Xiang <sup>2</sup>, Yuxuan Ying <sup>3</sup>, Yuqin Jiao <sup>4</sup>, Rui Zhao <sup>4</sup> and Waishan Qiu <sup>5,\*</sup>

<sup>1</sup> Royal College of Art, Wanqi.Shi@network.rca.ac.uk

<sup>2</sup> University College London, ucbq109@ucl.ac.uk

<sup>3</sup> Zhejiang University, 3170103432@zju.edu.cn

<sup>4</sup> UC Berkeley College of Environmental Design, yuqin62@berkeley.edu, rui\_zhao@berkeley.edu

<sup>5</sup> Department of Urban Planning and Design, The University of Hong Kong

\* Correspondence: waishanq@hku.hk

**Abstract:** Measuring and predicting Carbon Emission (CE) is important to enabling the main culprit of various urgent environmental issues including global warming. However, prior studies did not fully incorporate the impact of micro-level urban streetscapes, which might lead to biased prediction of urban CE. To fill the gap, we developed an effective framework to predict residential CE in urban areas from widely existing and publicly available street-view images (SVI) using machine learning. First, we used a semantic segmentation algorithm to classify more than 30 streetscape elements from SVI images to describe the built environment whose features might affect residential and transportation CE. Second, based on the streetscapes quantified, we trained a 10-fold cross-validation method with various machine learning models to predict the CE at the 1KM grid level using CE data from the PlanetData. We found first, built environment features such as sidewalks, roads, fences, buildings, and walls are significantly correlated with the residential CE. Second, the presence of buildings and subtle streetscape features (e.g., walls, fences) indicates higher-density residential areas which are related to more residential CE. Third, vegetation (e.g., trees and grass) are reversely related to residential CE. Our findings shed light on the feasibility of using a single and open data source (i.e., the SVI) to effectively model neighborhood-level CE for regions across diverse urban forms. Our framework is useful for urban planners to inform new town development and urban regeneration towards the low CE goals.

**Keywords:** carbon emission; residential; neighborhood level; street view images; machine learning; Beijing

## 1. Introduction

### 1.1. Urban Form and CE

Carbon emissions (CE) from fossil fuels (e.g., paraffin, gas, coal, and natural gas) have driven the global climate change (Du and Li, 2019; Qian *et al.*, 2022) which result in more frequent natural disasters (Shi *et al.*, 2022), causing societal crisis such as the insecurity in portable water (Huang and Tao, 2020) and energy (Ryu *et al.*, 2014). China, as one of the main emitters (Liu, Li and Ji, 2021), generates ~10 billion tons CE annually – roughly 1/3 of all nations (Joint Research Centre (European Commission) *et al.*, 2023). In reaction, China is committing to achieve the “3060” goal with CE reduction measures across many sectors (CSC, 2021; He, Liu and Wang, 2022). Notably, the residential sector is the second largest emitter which accounts for 23% of the Total Final Consumption (TFC) of fossil fuels (Fan *et al.*, 2013; Yuan, Wang and Zuo, 2013). Considering the rapid growth of urbanization, the numerous population of urban dwellers and the corresponding lifecycle energy

consumption of the residential buildings play a crucial role (Park and Heo, 2007; Baiocchi, Minx and Hubacek, 2010; Cao *et al.*, 2020).

Consequently, for China to successfully transit to a low-carbon economy, the neighborhood level CE reduction measures become essential (Cheng *et al.*, 2022). It's the basic spatial unit in China that includes urban dwellers, their traffics, industry productions – a microcosm of the urbanization process (Zhang, Song and Yang, 2021). Therefore, street block level urban form reflects a city's efficiency regarding the allocation and utilization of energy resources (Wang *et al.*, 2019).

Along this line, this study hypothesizes that the neighborhood level urban form directly and indirectly influences CE through its multi-dimensional variables such as the land use and building density. Fully understand the interlinkages between the two can inform a more sustainable urban development to achieve the reduction goal (Zheng *et al.*, 2023).

To understand how the urban form affect CE requires a capability to accurately model greenhouse gas concentration, as well as a comprehensive dataset to capture factors influencing CE at the individual and regional levels (Kumar *et al.*, 2023). However, it has long been challenging to model the complex urban environmental phenomena which are highly variable in time and space (Jordan and Mitchell, 2015; Helm *et al.*, 2020). Specifically, this study aims to tackle with the following three gaps.

### 1.2. Knowledge Gap

First, the data sources for CE models are limited. Traditionally, predicting residential CE relies on multifaceted GIS data – the energy-consumption as well as socioeconomic and demographic datasets (e.g., the census, the household economics survey) to build a regression model. However, detailed energy consumption data are not available in many cities – it does not even exist for some small cities due to the deficiency of funding for CE data collecting; nor do fine-grained population data exist everywhere (Cai *et al.*, 2021), other data related to energy consumption are often only at the city scale rather than at the mesoscale (Du, Liu and Li, 2024). Additionally, another challenge is that socio-economic data are usually on the different time scale with the energy consumption data. Therefore, conventional CE prediction models are not immediate applicable to a new region nor a different period (Zheng *et al.*, 2022).

Second, the accuracy is often limited, given the increased complexity of urban form variables. Oftentimes, multiple sources are deployed to generate the multifaceted independent variables (e.g., land use, residential density, travel mode choice, traffics). However, the built environment and the corresponding residential activities are perpetually evolving such that the dataset for some variables will not be up-to-date (Ou *et al.*, 2013, 2019; Fang, Wang and Li, 2015; Shu *et al.*, 2018; Wang *et al.*, 2019; Shi *et al.*, 2020; Qiu *et al.*, 2023). That said, building a timely-effective model at the urban scale is desirable however difficult. By contrast, street view imagery data (SVI) which is frequently updated and open source (Qiu *et al.*, 2022; Dong *et al.*, 2023, 2023; Su, Li and Qiu, 2023), can describe the timely changes of the built environment at least on a yearly basis. In addition, scholars use complex data sources hoping to cover more social situations related to carbon emissions, but this does not mean better model accuracy, it can be counterproductive (Bolón-Canedo and Remeseiro, 2020; Kabir and Garg, 2023).

Third, the traditional model is generally built based on satellite image and GIS data that ignoring the street-level information which is more capable to model neighborhood-level activities that consume fossil energies. For example, satellite image is not fully capable to describe the urban form at a fine granularity – there are just many sight obstructions, e.g., tree canopy or the view angles. Taking transportation CE (Xia *et al.*, 2020) as an example, driving trajectory data is often the source of insight to estimate traffic flows and the corresponding CE. However, satellite images lack the traffic information for many residential blocks due to the obstructions from tree canopies. While SVI is capable to infer traffic information for the neighborhoods, therefore is promising to improve the accuracy of CE modeling.

### 1.3. Hypothesis and Research Design

The built environment consists of various factors that influence residential CE (Shen *et al.*, 2022), ranging from the urban greening (Vaccari *et al.*, 2013; Shen *et al.*, 2022; Dong *et al.*, 2023), density (Liu *et al.*, 2019), building height and building quality (Tranchard, 2017), to the public infrastructures (e.g., road, bus stop) (Zhang *et al.*, 2020). Notably, most of the factors can be extracted from SVIs. For example, the green view index is a proxy of the greenery (Lu *et al.*, 2023) which is important to carbon sequestration (Dwyer *et al.*, 2000; Nowak and Crane, 2002; Birge *et al.*, 2019), while the building view index is a proxy to building density and building height (Carrasco-Hernandez, Smedley and Webb, 2015; Gong *et al.*, 2018) that significantly affect CE (Resch *et al.*, 2016). The adequate public infrastructure and convenient transportation (e.g., road, streetlights, bus stop) may suggest a more walkable and bikeable neighborhood whose residents would have higher tendency for active travel (Li and Joh, 2017; Dong *et al.*, 2023), resulting in lower CE (Zhang *et al.*, 2020). A more developed economy with adequate infrastructure also relates to better maintained buildings whose dwellers exhibit stronger awareness and obligation of low-carbon measures. For example, the streetscapes such as wall and fences can imply the quality of the building – a more complex composition of the façade suggests a higher quality building whose likelihood of HVAC installation is higher – and whose residents' income is higher, tending to consume more energy. In other words, streetscape features extract from SVIs can imply abundant dweller behavior information which can outweigh the impacts of the geometry itself to model energy use (Quan *et al.*, 2016).

The micro-scale built environment described by SVI is also related to other indicators of residential behaviors, including walkability (Ha *et al.*, 2023), bikeability (Ito and Biljecki, 2021; Qiu and Chang, 2021; Song *et al.*, 2023), running (Dong *et al.*, 2023), public transit ridership (Su *et al.*, 2022), therefore the mode choice (Koo *et al.*, 2023; Wu, Yao and Wang, 2023) and active living (Sallis *et al.*, 2006; Steinmetz-Wood *et al.*, 2019). Moreover, SVI can infer the urban forms like street canyons and density (Middel *et al.*, 2019; Qiu *et al.*, 2021) that explains local climate zones (Cao *et al.*, 2022; Ignatius *et al.*, 2022; X. Xu, Qiu, Li, Huang, *et al.*, 2022) – an effective indicator for modeling neighborhood microclimate, outdoor comfort, and urban heat island effects (Stewart and Oke, 2009, 2012; C. Xu *et al.*, 2022) which ultimately influence energy usage and CE.

In terms of the feasibility of SVI data source, Google provide publicly available API access to obtain the frequently-updated SVIs, while Baidu and Tencent are dominant suppliers in China. SVIs have become a common method to replace the time-consuming and costly field auditing (Rundle *et al.*, 2011; Griew *et al.*, 2013; Kelly *et al.*, 2013; Queralt *et al.*, 2021), being easily implementable at the urban scale (Salesses, Schechtner and Hidalgo, 2013; Dubey *et al.*, 2016). However, despite SVI's large potential, little has been empirically tested to justify its effectiveness. To fill in the gap, this paper proposes an image-based framework to directly predict residential CE based on the micro-level streetscape features extracted from SVI dataset.

## 2. Literature Review

### 2.1. Conventional Urban Energy Models

Conventional urban CE models can be classified into three families based on methodology: 1) models directly measure the CO<sub>2</sub> concentration from remote sensed satellite data, for example, the TanSat Satellite (Hong *et al.*, 2022); 2) models aggregate sectoral emission data collected from sensors monitoring viable spatial grids ranging from a city to a household, among which “one square kilometer” is the most common resolution (Gregg and Andres, 2008); 3) models relate the global CE data to human societal indicators in smaller spatial units (Huang *et al.*, 2022).

The first approach mainly translates observed spectral data into the distribution of carbon dioxide, thereby obtaining global or regional scale carbon flux information. It becomes a key source for observing global and regional CO<sub>2</sub> distribution (Crisp, 2010; Yoshida *et al.*, 2011). Publicly accessible satellite datasets include the Europe's SCIAMACHY, the USA's OCO-2 and OCO-3, Japan's GOSAT and GOSAT-2, and China's TanSat (Hong *et al.*, 2022). Recent studies have showcased the capability to map and estimate regional CO<sub>2</sub> emissions (Hakkarainen, Ialongo and Tamminen, 2016) as well as facility-scale CH<sub>4</sub> fluxes in urban and complex areas (Thompson *et al.*, 2016;

Frankenberg and Berry, 2018). This method exclusively yields CO<sub>2</sub> emission data based on advancements in satellite technology, its disadvantages are as evident as its merits: it offers frequent updates for the global coverage in atmospheric CO<sub>2</sub> levels.

The second approach collect carbon data from sensors (Christen, 2014; Feng *et al.*, 2016) or simulated energy consumption and CE (Pao and Tsai, 2011) including the fuel consumption conversion based on prior sensor data (Shao *et al.*, 2016). It often determines the total CE of a given region based on fossil energy consumption information disaggregated by sectors – this is particularly prevalent in China. For example, China's National Greenhouse Gas Inventory is a created by experts from various fields with the National Development and Reform Commission. They developed the "Provincial Greenhouse Gas Inventory Compilation Guidelines (PGGICG)" in 2011, comprising sectors including waste disposal, land-use changes, forestry, agriculture, production processes, industrial and energy activities. In the US, (Gurney *et al.*, 2019) quantified CE from all fossil fuel consumptions by sector with a bottom-up method – hourly emissions from citywide industrial/electricity facilities, road segments and individual buildings were measured. Notably, various datasets, such as building energy simulations, electricity production data, traffic insights, and local pollution reports were merged to build the dataset. City sub-regions can also be modeled. For example, (Wu, Guo and Peng, 2003) measured the energy use intensity (EUI) for each building type using the building energy efficiency monitoring platform in Shanghai. (Zhang, Pu and Zhu, 2013) incorporated a traffic allocation model to mimic traffic situations using a gasoline consumption function – the User Equilibrium (UE). Although their method versatility suits major cities in the more developed world, it's not immediately applicable to medium to small size cities in many developing countries where no similar data source exists.

The third approach disaggregate global CE data to a finer resolution relating to the indicators describing the built environment and industrial activities. It's because there was a strong alignment between surface fluxes of atmospheric CO<sub>2</sub> and bottom-up inventories (Schuh *et al.*, 2013; Ogle *et al.*, 2015) or urban activities indicators like land use (Jain, Meiyappan and Richardson, 2013; Chuai and Feng, 2019) and road length (Song *et al.*, 2021). On the one hand, nighttime light (NTL) image is found to reflect human activities correlated with energy consumption. Therefore, the brightness of NTL pixels significantly correlates with CE, enabling the prediction across spatial and temporal scales. On the other hand, various urban layers, such as transportation network (Ehsani, Ahmadi and Fadai, 2016; Sun *et al.*, 2017), buildings (Boehme, Berger and Massier, 2015; Peng, 2016; Ahmad *et al.*, 2018), and households (Pachauri, 2004; Druckman and Jackson, 2008) were related to the CE prediction (Kaya, 1989). Others explanatory factors include population (Ribeiro, Rybski and Kropp, 2019) and living standards (Baiocchi, Minx and Hubacek, 2010). This approach is particularly useful for alternative urban scenarios' ex-ante assessment to support decisions like urban retrofit aiming at achieving low carbon goals (Gately and Hutyra, 2017; Zhang, Song and Yang, 2021).

## 2.2. Street View Image and AI to Model Urban Forms

Multifaceted natural, socio-economic, and human behavior forces have made the neighborhood level residential CE prediction challenging (Berkhout, Hertin and Jordan, 2002). Fortunately, With the rapid improvements of AI and multi-source big data application for urban studies, many urban form characteristics that are used to model CE become more accessible for researchers (Li *et al.*, 2022). Some focus on the complex relationships between total urban CE and the industrial/economic development level or urban sprawl trend of the region (Du *et al.*, 2018; Wen and Shao, 2019). Some other studies consider the regularity of historical data (Zhou *et al.*, 2021) – the cyclical trends in CE. For example, (Wilson and Dowlatabadi, 2007) studied the influence of household members' environmental perceptions and the energy consumption behavior on household CE. More recently, (Jiang *et al.*, 2019) model household travel patterns from neighborhoods' urban forms to evaluate CE. Increasing number of models start to address the interplay between people's energy use habits and the environment they live in.

Meanwhile, SVI data is publicly available and frequently updated to capture ground-level panorama street scenes (Seiferling *et al.*, 2017). SVI is an ideal dataset to comprehensively describe

the urban environmental variability. For example, it has been used to model buildings (Gurney *et al.*, 2012) including building height (Yan and Huang, 2022), streetscape features (Wang, Liu and Gou, 2022), green and water systems (Jiang, Jiang and Shi, 2020), land use classification (Jain, Meiyappan and Richardson, 2013; Tian, Han and Xu, 2021; Fang *et al.*, 2022), the openness (Xia, Yabuki and Fukuda, 2021), road network (Zhang *et al.*, 2023), mobile monitoring (Sun *et al.*, 2017) and POI (Gao, Janowicz and Couclelis, 2017; Huang *et al.*, 2022; Song *et al.*, 2022; X. Xu, Qiu, Li, Liu, *et al.*, 2022). However, as a new dataset receiving a lot of attention in urban studies, only few studies attempted to parse SVIs to reflect the state of urban CE. For example, (Yu *et al.*, 2022) considered SVIs as one of the data sets to model household travel CE in Jinan, China. However, SVIs only represent the road and road-building relationship (i.e., urban canyon) in their model. To fill in the gap, this study sets to address the effectiveness of using SVI data to represent urban forms relate to the energy use behaviors of residents, to predict the residential CE.

### 3. Data & Method

#### 3.1. Study Area and Analytical Framework

##### 3.1.1. Study Area

Beijing, as the capital city and one of the largest metropolitans in China, is crucial to address the CE reduction goal. Moreover, its diverse urban forms ranging from CBD, residential blocks, industry parks to periphery, with its massive road network, provide important samples to address the effectiveness of our proposed framework. Within the Sixth Ring Road is the area where the majority urban residents live in. This region serves most frequent urban mobility and resident activities. Therefore, the area within the Sixth Ring Road in Beijing is chosen (Figure 1.)

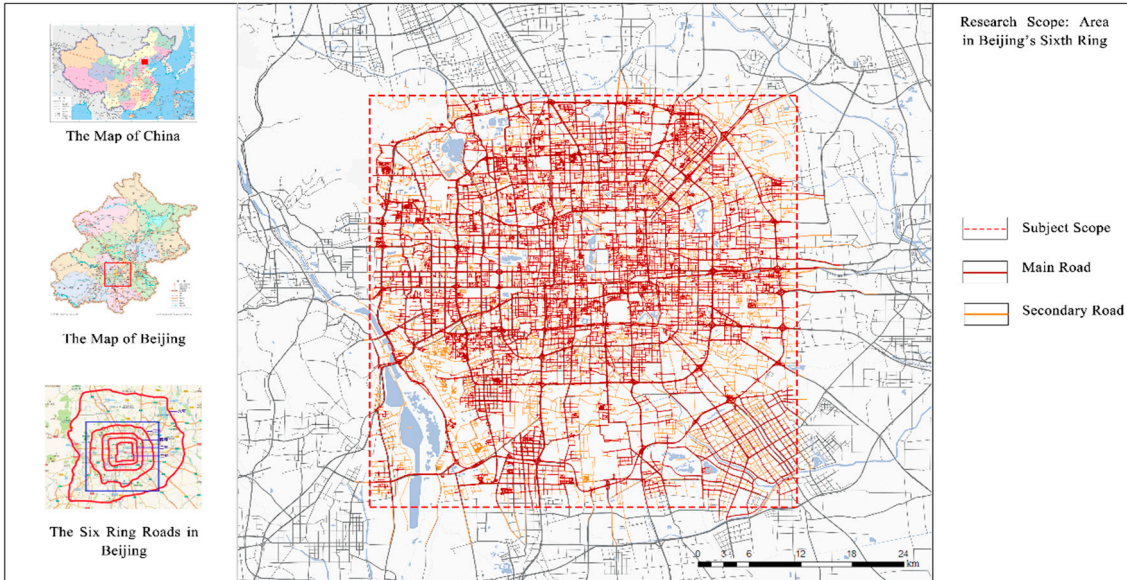
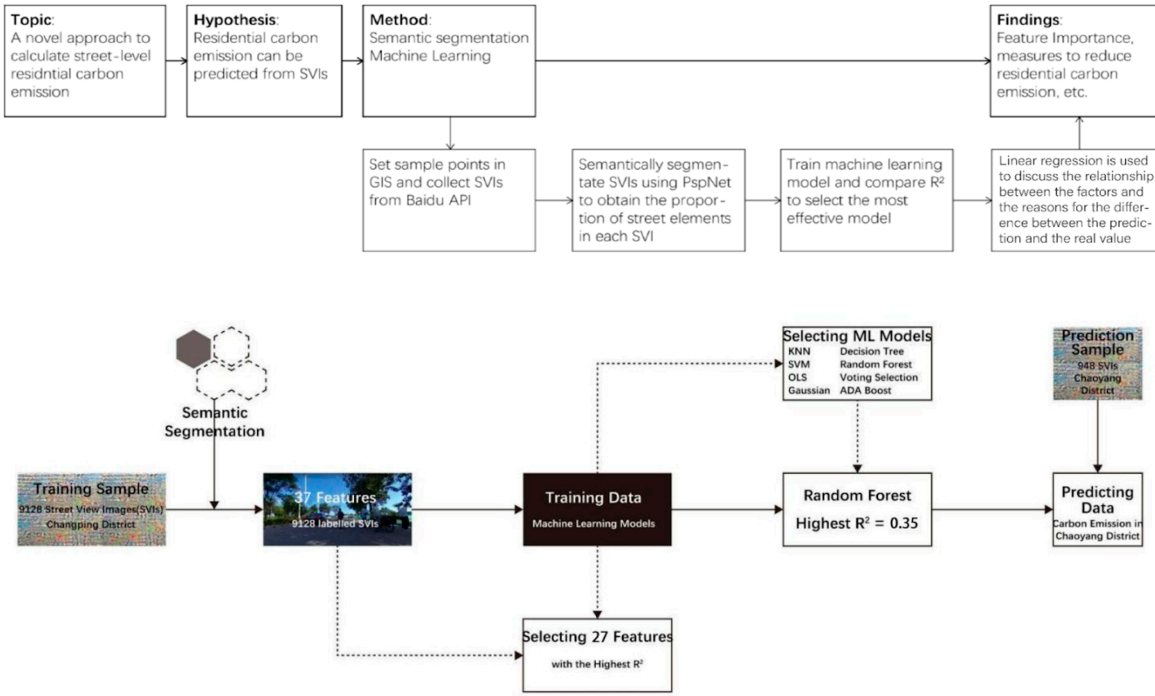


Figure 1. Study Area: Beijing.

##### 3.1.2. Conceptual framework

Our model framework consists of six steps (see Figure 2). First, remote sensing CE data are collected from PlanetData (<https://www.planet-data.cn/>), with a surface data grid of 1km\*1km. Second, obtaining the SVI of the selected point by using Baidu API (<https://lbsyun.baidu.com/>) in Python through the coordinates of the selected points along the road network in Beijing at a 250-meter interval. For each sampling coordinate, we obtained the 360 degree-view SVI. Third, PSPNet, a semantic segmentation model was used to extract the proportion of various street elements from each SVI. The top xx most ubiquitous visual elements related to CE suggested by literature, including the surface, sidewalk, greenery, sky, road, building, wall, fence, and seat are selected. Forth, training

ML models to predict CE using visual features extracted in Python. The goodness of fit ( $R^2$ ) was chosen as the criteria to select the most accurate models from the four ML models (i.e., KNN, SVM, random forest and decision trees). Last, we use the trained ML model to predict the residential CE in Beijing, visualizing the gaps between the ground truth CE and our best prediction, to validate our model and understand the potential causes of the biases.



**Figure 2.** Analytical Framework.

### 3.2. Variables

#### 3.2.1. Residential Carbon Emission

The residential CE in July 2021 in Beijing is collected from the PlanetData (<https://www.planetdata.cn/>, 2022, accessed April 2022) – a carbon data provider who provides the tagged image file (TIF) of residential CE in 1KM city grid. The raw data from the Tsinghua University MEIC CE data inventory. By relating urban activity indicators (e.g., energy consumption and the number of residents per area) with the original satellite CE data (at the 1/4° resolution), PlanetData established a 1KM resolution model (1/100°) covering the entire China using a fusion model. Since the focus of this paper is to demonstrate the usefulness of predicting CE from SVI, we randomly choose a month data in the most available year in Beijing as the case study (Figure 3).

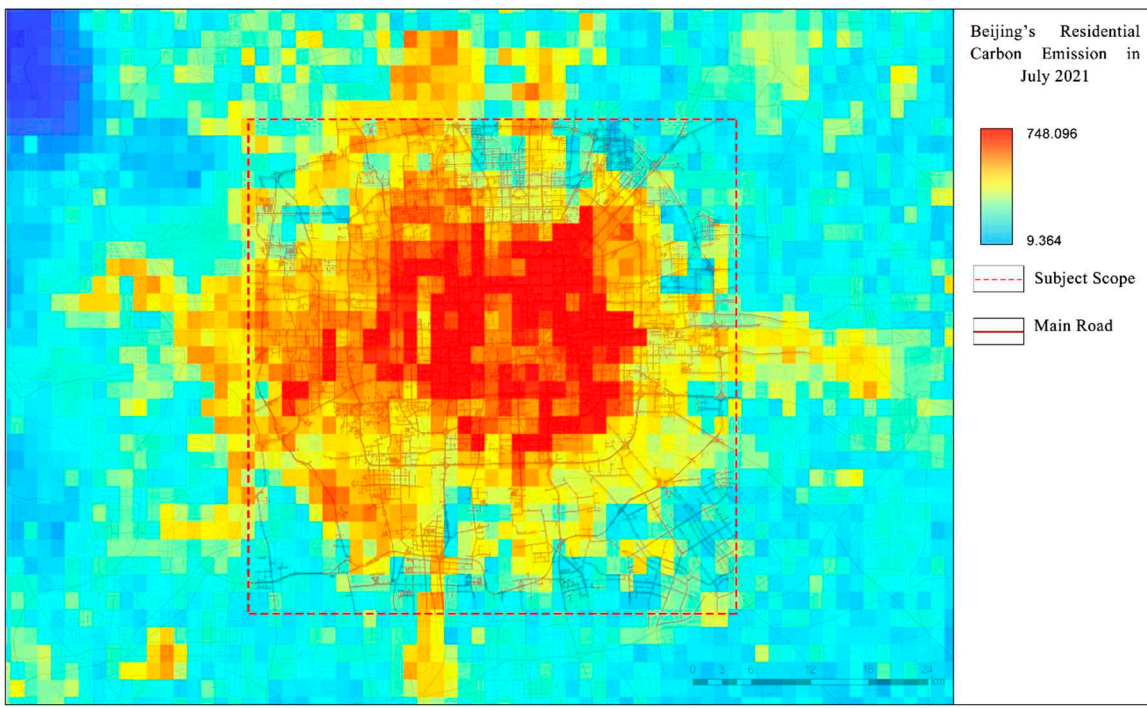


**Figure 3.** Beijing's Residential CE in July 2021.

### 3.2.2. Independent Variables

#### 3.2.2.1. SVI Data Collection

The panoramic SVI dataset was downloaded with the Baidu Map Open-Platform (i.e., the Baidu API: <http://api.map.baidu.com/panorama/v2>) between April-May 2022. The sampling interval is every 250 meters along the road networks (Figure 4). The panorama photos include street views from all four directions at each sampling point. Note that (by checking the meta data) all SVI samples were taken during 2019-2021 – being the most up-to-date dataset that available to match the period of our CE data. We looked through the street-view history in Baidu Map, which make it possible that users could see how a place has changed over the years and help on identifying changes in the physical environment, and there were few major construction projects in the study area during this period. Considering the street environment is rather stable in a short term (Liang, Zhao and Biljecki, 2023), we were able to assume no significant changes happened between the sample period (2019-2021). Notably, the SVI retrieval process is also consistent with all parameters including the heading, the position coordinates (longitude and latitude), the image resolution (width and height), the horizontal field, and the pitch. In total, 25,046 images were downloaded for the study area.

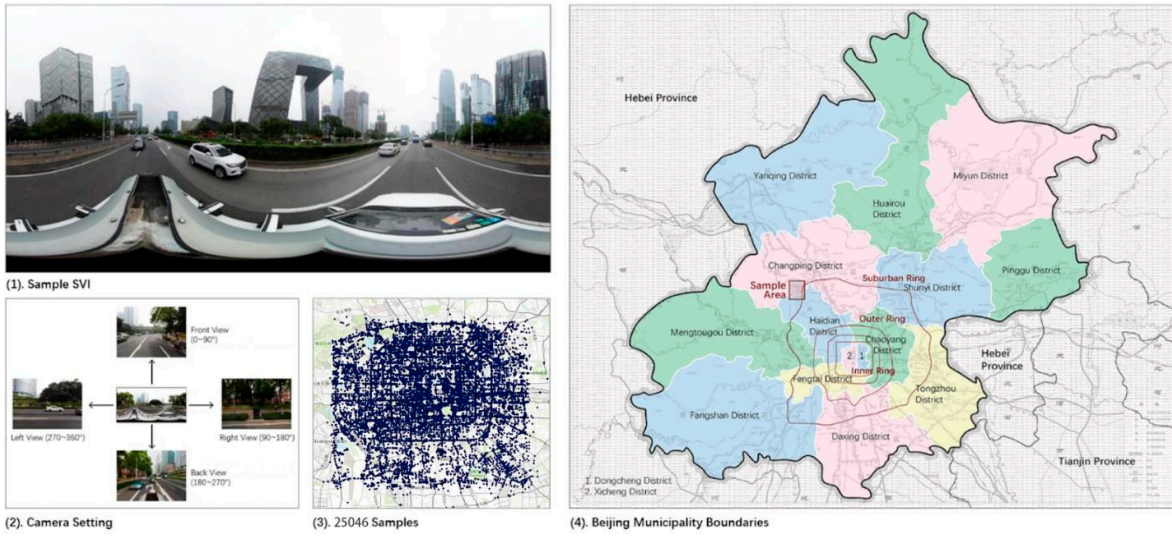


**Figure 4.** SVI Samples.

### 3.2.2.2. Semantic Segmentation

The independent variables are streetscape visual features extracted from the 25,046 SVIs (Figure 4). Streetscape features representing the micro-level-built environment that becomes hidden layers to represent comprehensive urban information related to residential CE, such as its urban location, land use, microclimate condition, residents' behavior such as their living styles and habits which link to the residential CE.

PSPNet (Pyramid Scene Parsing Network), a deep learning (DL) semantic segmentation was used to process SVIs. Semantic segmentation refers to dividing and parsing images into several areas linked with semantic categories (Guo *et al.*, 2018). The PSPNet has become a commonly used approach by emerging urban studies to extract street canyon characteristics (Zhao *et al.*, 2017; Yuan, Wang and Xu, 2022; Sun *et al.*, 2023) and shown state-of-the-art performance on the ADE20K database, achieving an accuracy of over 80% (Zhao *et al.*, 2017; Zhou *et al.*, 2019).

Consequently, for each SVI, the output is the visual feature's view index – denoting as the pixel percentage of the feature identified to the total pixels of the image. More than 50 visual features were observed from all SVI samples in Beijing (Figure 5), including natural features (e.g., trees, grass), built environment features (e.g., roads, sidewalks, buildings), and traffic features (e.g., cars, buses, bicycles). Evidently not all visual elements should be taken as the independent variables. Variables whose presences in SVIs were minor (e.g., sculpture, lamp, fountain, pier, van, minibike) were removed.

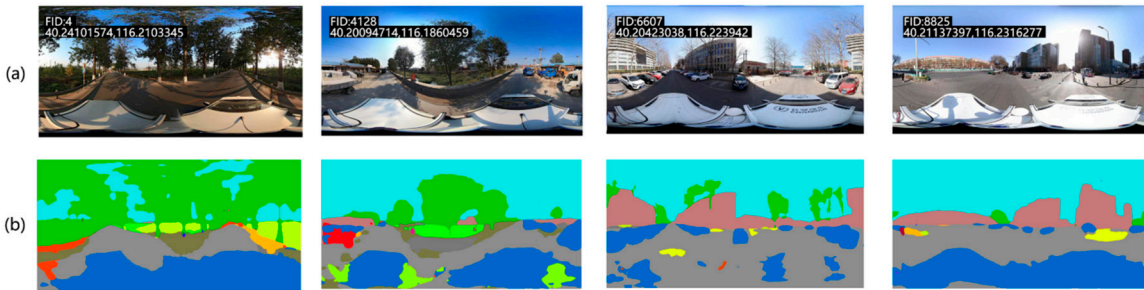


**Figure 5.** SVI Semantic Segmentation.

To this end, the residential CE at each SVI sample point becomes the dependent variable, while the selected visual features' view indices become the independent variables for all the 25,046 SVI to train the ML models for prediction.

**Table 1.** Summary of streetscape visual elements.

Variables		Mean	Min	Max	Std Dev.	Data Source
Y	Carbon emission	688.20	1.14	1914.87	487.97	Planetdata.com
X1	wall	83.55%	10.00%	99.98%	24.70%	
X2	building	19.23%	10.00%	99.99%	26.49%	
X3	sky	52.24%	11.00%	100.00%	12.38%	
X4	tree	59.53%	10.00%	100.00%	24.92%	
X5	road	15.44%	10.00%	99.97%	17.71%	
X6	grass	34.38%	10.00%	99.99%	23.99%	
X7	sidewalk	74.60%	10.00%	99.98%	24.48%	
X8	person	45.75%	10.00%	99.98%	24.39%	
X9	earth	28.70%	10.00%	99.98%	25.29%	
X10	car	16.34%	10.00%	100.00%	24.58%	
X11	fence	16.85%	10.00%	99.97%	24.81%	
X12	railing	65.90%	10.00%	99.96%	24.51%	
X13	column	49.67%	10.00%	99.99%	24.64%	
X14	bridge	11.64%	10.00%	99.98%	25.06%	
X15	streetlight	23.65%	10.00%	99.98%	24.96%	
X16	plant	22.61%	10.00%	99.96%	25.05%	
X17	signboard	73.56%	10.00%	99.90%	24.76%	25,046 panorama
X18	minibike	16.17%	10.00%	99.91%	24.41%	SVIs in Beijing
X19	chair	16.57%	10.00%	99.95%	24.74%	
X20	bicycle	16.97%	10.00%	99.90%	24.38%	
X21	lamp	13.16%	10.00%	99.99%	24.86%	
X22	van	11.27%	10.00%	99.91%	24.89%	
X23	ashcan	92.73%	10.00%	99.90%	24.73%	
X24	skyscraper	12.30%	10.00%	99.98%	24.91%	
X25	ceiling	19.77%	10.00%	99.80%	24.67%	
X26	mountain	14.22%	10.00%	99.90%	24.29%	
X27	awning	17.25%	10.00%	99.83%	24.09%	
X28	windowpane	12.16%	10.00%	99.50%	24.71%	
X29	sculpture	19.86%	10.00%	99.98%	25.01%	
X30	fountain	14.18%	10.00%	99.70%	24.59%	
X31	water	15.15%	10.00%	99.80%	24.61%	
X32	pier	23.82%	10.00%	99.90%	25.85%	
X33	sofa	16.38%	10.00%	99.60%	25.19%	
X34	bulletin board	21.81%	10.00%	97.00%	23.66%	

X35	booth	15.11%	10.00%	89.56%	21.14%
X36	glass	24.95%	10.00%	90.00%	30.91%
X37	desk	46.43%	10.00%	91.00%	25.19%

### 3.3. Model Architecture

#### 3.3.1. Machine Learning Models

Regarding the ML training, 80% of the sample was used for training, and 20% for validation. The training utilizes a ten-fold cross-validation approach was deployed to add the effectiveness of models' training. Specifically, dividing the input data into 10 subgroups: for each iteration, one subgroup is utilized as the testing data while the other nine subgroups are employed for training. In other words, all data is utilized to train the ML models after 10 iterations – lowering the bias. What's more, every iteration's model weights for the convolutional layers are continuously updated, which also adds the effectiveness of training (Malakouti, 2023).

#### 3.3.2. Model Selection

Since the number of independent variables are less than 40, we excluded the neural network model. Eight commonly used ML models were selected to train the data based on literature regarding the model's usefulness in predicting continuous variables related to urban studies (Table 2).

**Table 2.** Comparison of ML model performance.

Index	Model	R <sup>2</sup>	RMSE (t/km <sup>2</sup> /months)	MAE (t/km <sup>2</sup> /months)
1	KNN	0.35	105.17	83.21
2	SVM	0.1	123.31	100.61
3	Random Forest*	0.80	58.11	40.90
4	Decision Tree	0.74	66.79	21.69
5	OLS	0.1	123.04	100.22
6	Gaussian	0.0	130.72	106.64
7	Voting Selection	0.47	95	77.11
8	Gradient Boosting	0.23	113.97	93

Note: \* The best model selected.

For example, the Random Forests (RF) which has been tested by many prior urban studies. The accuracy of ML models was evaluated using the R<sup>2</sup> (correlation coefficient), RMSE (root mean square error), MAE (mean absolute error), and IA (index of agreement). Whereas R<sup>2</sup> represents the goodness of fit, IA is representative for the agreement of the estimated value with the observed value, and the fitting effect of MAE and RMSE is representative for the deviation of the estimated value from the observed value.

To enhance the quality of our dataset and to ensure robust analysis, we employed a method to identify and remove outliers from the SAMPLE residential column – the Interquartile Range (IQR), a common statistical approach for outlier detection. Instead of the traditional 25th (Q1) and 75th (Q3) percentiles, we opted for the 30th and 70th percentiles to compute the IQR. After the outlier removal process, approximately 99.57% of the original data remained. This process ensured that our analyses were conducted on a dataset free from extreme values that might skew the results.

As an initial test, we first selected top 10 ubiquitous visual elements (e.g., 'sky', 'person', 'earth', 'car' 'sidewalk', 'grass', 'road', 'tree', 'building', 'wall') as training inputs, which resulted in an R2 of 0.78505 as the baseline model. We then selected 27 elements excluding almost-all-zero-ratio visual elements and obtained an R2 of 0.80021 (best model). Notably, when tested with all visual elements, the models obtained an R2 of 0.80015, whose effectiveness is next to the best model. Random Forest was finally selected for the final validation.

## 4. Results and Discussions

### 4.1. Spatial and Temporal Distribution of Residential CE in Street Microenvironment

In general, high values of CE happen in densely populated area such as the center of the city. The CE of residents in diverse microenvironments show significant spatial heterogeneity. For example, the unit CE of suburban areas around Beijing are the lowest, with the CE in July ranging from 106 to 211 t/km<sup>2</sup>/months, while the unit CE are higher when closer to the center of the city where the density of residents is high. The CE in July is between 950-1,056 t/km<sup>2</sup>/months. In the eastern urban districts of Beijing, such as Chaoyang and Dongcheng, the overall CE in residential area in summer are higher than those in the western urban districts, such as Changping and Haidian. This is probably because the eastern urban area is an old urban area, with more residents' activities and a higher population density, resulting in more CE.

Therefore, the CE in Beijing residential area presents spatial heterogeneity distribution obviously. Meanwhile, the density of residents and their activity frequency can be directly reflected from the street view. That's because residents' activities largely shape the street view images. For example, in general, a place with a higher population density has more residents' activities, more residential buildings and higher building density, which then demonstrates as less greenery and more bounding walls. In addition, a place with more residents' activities and more population has more vehicles in the street view images. Therefore, the street map can be used to predict residents' CE and reflect the spatial heterogeneity of residents' CE accordingly.

### 4.2. Co-linearity Check for the Independent Variables

We plotted the heatmap of pairwise correlation coefficients (Figure 6) to show the relationship between the streetscape visual features to examine the potential co-linearity issues. Highly correlated variables will be further discussed with reference to Importance Features (IF) score and theory to decide whether to be removed to reduce the redundancy. For example, our results show that "earth" and "road" are highly related to prompt concerns about potential redundancy. However, in this case, both "earth" and "road" are important as they indicator different aspects affecting the residential energy use: while "road" indicate travel models and mobility/accessibility related to travel frequency, earth can affect permeability of the land surface and the micro-climate. Therefore, both were kept.

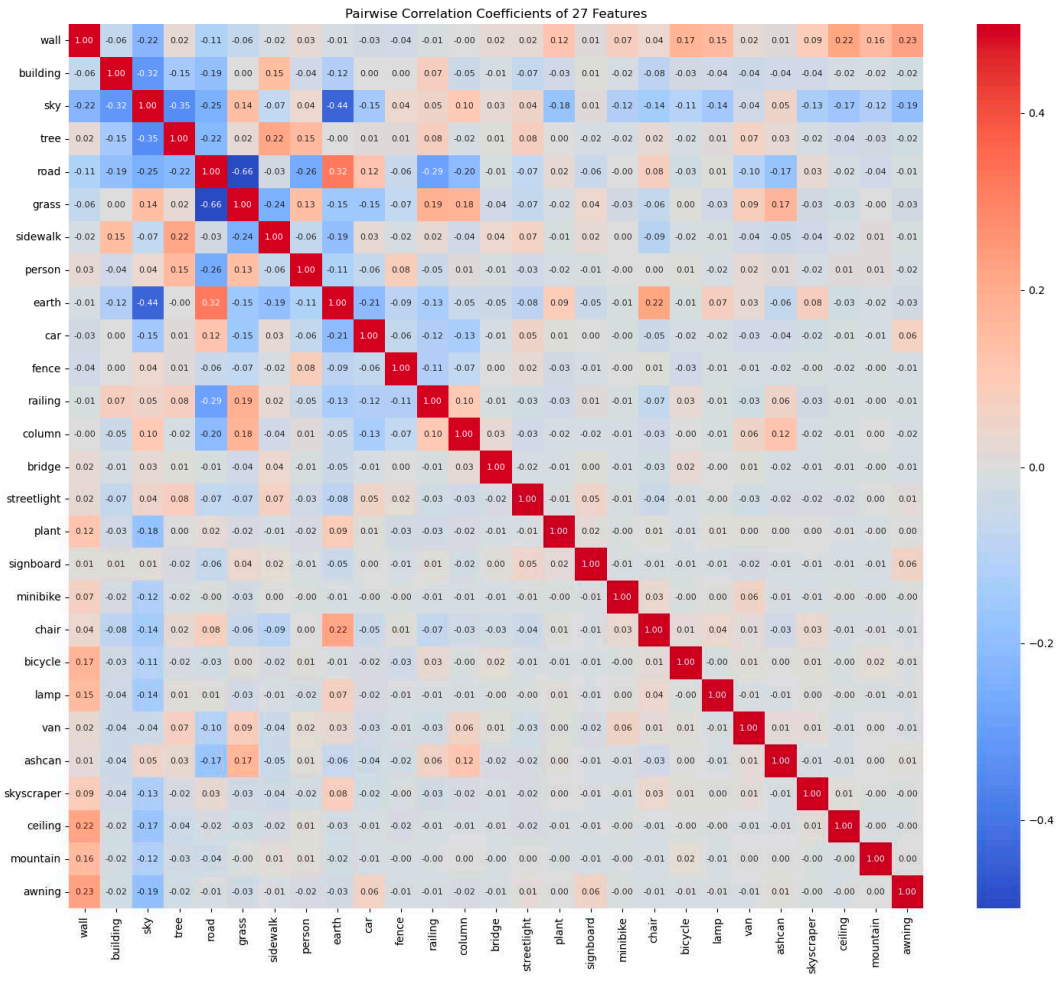


**Figure 6.** Pairwise Correlation Coefficients of 27 Features.

#### 4.3. The Roles of Micro-Level Built Environment Visual Features

The impact factor (IF) and feature importance (FI) analysis reveal big divergence regarding what visual features are more important determinants in predicting the CE. On the one hand, the IF ranking based on linear regression coefficients indicates that the bridge, streetlight, van, signboard, ashcan, chair, minibike, grass, earth, railing was the most impactful (Figure 7). On the other hand, the FI analysis, by contrast, highlights divergent visual elements are more effective when using tree-based ML models (Figure 8). The top 10 features regarding FI are earth, sidewalk, tree, sky, road, building, fence, wall, chair, and grass. Given the OLS has a significant poorer performance (Table 2), the relationship between visual features and the CE is more likely to be non-linear. The FI analysis is more reliable.

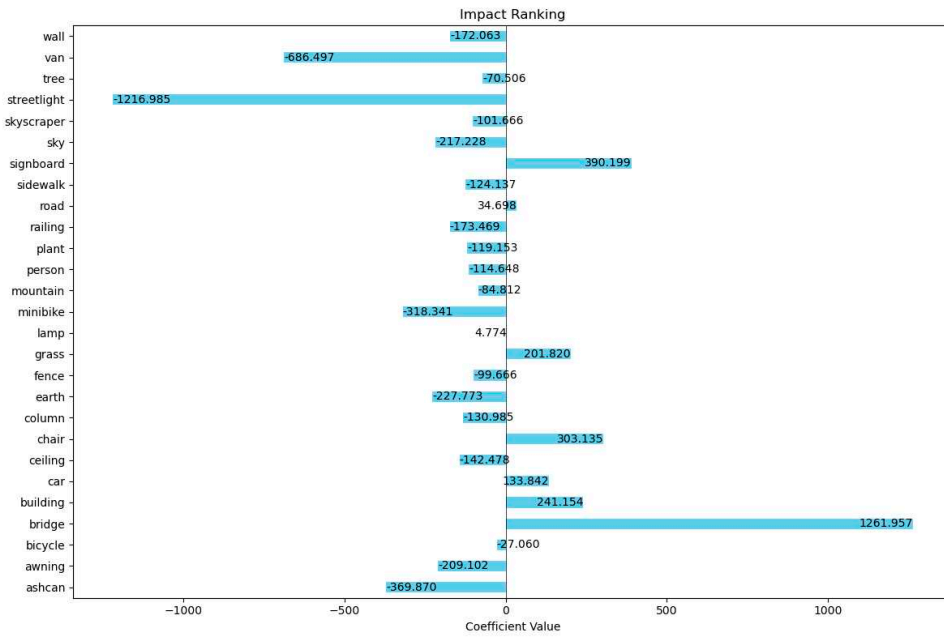


**Figure 7.** Impact Ranking based on linear regression model coefficients.

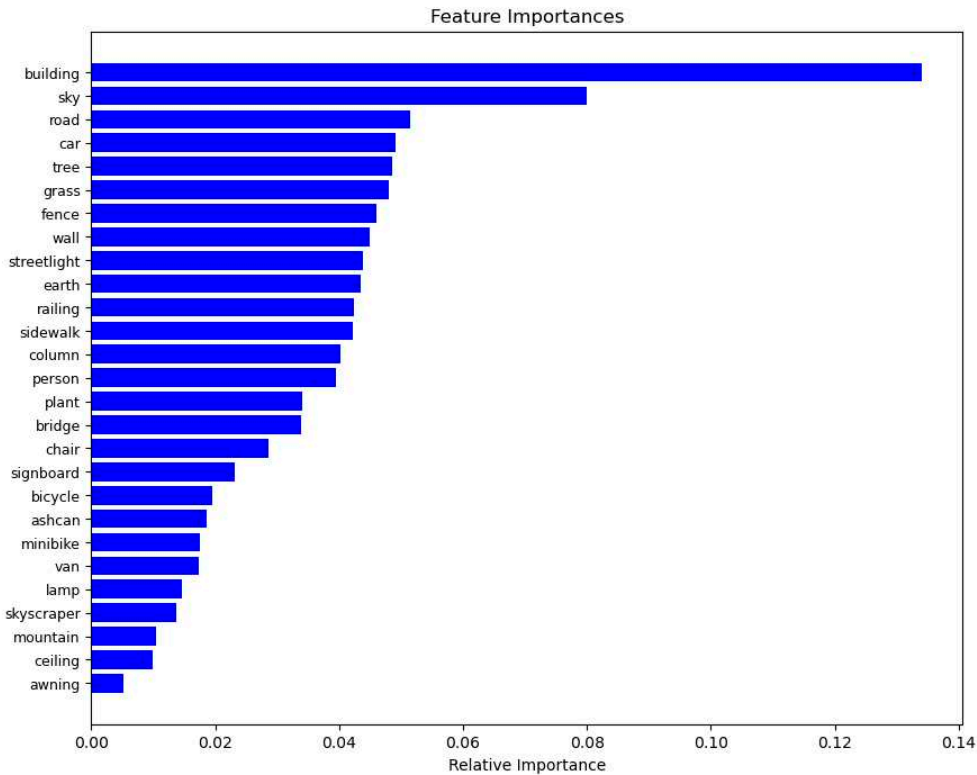


**Figure 8.** Feature Importance.

The Pearson Correlation analysis shows that built environment features such as sidewalk, road, fence, building, and wall are in strong correlation with residential CE (Table 3). One possible explanation for this result is that the high ratio of these elements means the high density of residents in the area, which results in the high frequency of activities that emit carbon and other greenhouse gasses. For instance, the high ratio of buildings in SVIs might indicate the high frequency of usage of air-conditioners in the buildings near the streets. Such a phenomenon is even more obvious in this study since the data of CE used in our model was collected in July, the time when the monthly average

temperature in Beijing was 29°C and air-conditioners and other household appliances were widely used. The high density of residents will also lead to a growth in the frequency of vehicle use. Therefore, the factor of road also indirectly determines the CE of the area, the higher the traffic volume, the larger the CE in the site.

**Table 3.** Pearson Correlation of selected dependent and independent variables.

	CE	wa ll	sk y	tre e	roa d	gra ss	sidew alk	ear th	pers on	pla nt	cha ir	car	wat er	fen ce	build ing
CE	1.0 0														
wall	- 0.0 3	- 1.0 0													
sky	- 0.0 2	- 0.1 2	1.0 0												
tree	- 0.0 1	- 0.0 1	0.8 7	1.0 0											
road	- 0.0 2	- 0.1 0	0.4 1	0.6 9	1.0 0										
grass	- 0.0 2	- 0.0 3	0.6 9	0.7 3	0.5 4	1.0 0									
sidew alk	- 0.0 4	- 0.0 3	0.2 8	0.1 8	0.1 3	0.1 6	1.00								
earth	- 0.1 1	- 0.0 2	0.1 6	0.1 5	0.1 2	0.0 6	0.03	1.0 0							
perso n	- 0.0 0	- 0.0 1	0.1 2	0.0 7	0.0 3	0.1 3	-0.02	0.1 3	1.00						
plant	- 0.0 2	- 0.0 0	0.2 2	0.2 6	0.2 9	0.1 9	0.11	0.1 5	-0.06	1.0 0					
chair	- 0.0 6	- 0.0 6	0.3 9	0.3 8	0.2 0	0.3 0	-0.04	0.0 1	-0.03	0.1 4	1.0 0				
car	- 0.1 1	- 0.0 6	0.2 6	0.2 3	0.1 2	0.2 5	-0.19	0.6 2	-0.09	0.0 7	0.1 1	1.0 0			
water	- 0.0 1	- 0.0 1	0.0 1	0.0 0	0.0 5	0.0 1	-0.03	0.0 2	-0.01	0.0 4	0.0 2	0.0 8	1.00		
fence	- 0.0 3	- 0.0 3	0.3 0	0.4 4	0.2 8	0.3 3	-0.16	0.0 4	-0.02	0.1 4	0.2 3	0.0 7	-0.01	1.0 0	
buildi ng	- 0.1 2	- 0.0 1	0.0 0	0.0 9	0.1 2	0.0 7	-0.05	0.3 5	-0.07	0.0 4	0.0 9	0.3 6	-0.01	0.0 8	1.00

In addition, better infrastructure (e.g., walls, fences) exists in higher-density residential areas. Elements like walls, fences and buildings might reduce wind speed and slow down the diffusion of carbon-containing gasses, thus keeping the carbon content in the streets at a relatively higher level than those in open streets with few obstacles. Meanwhile, (Choi *et al.*, 2016) found that the block-

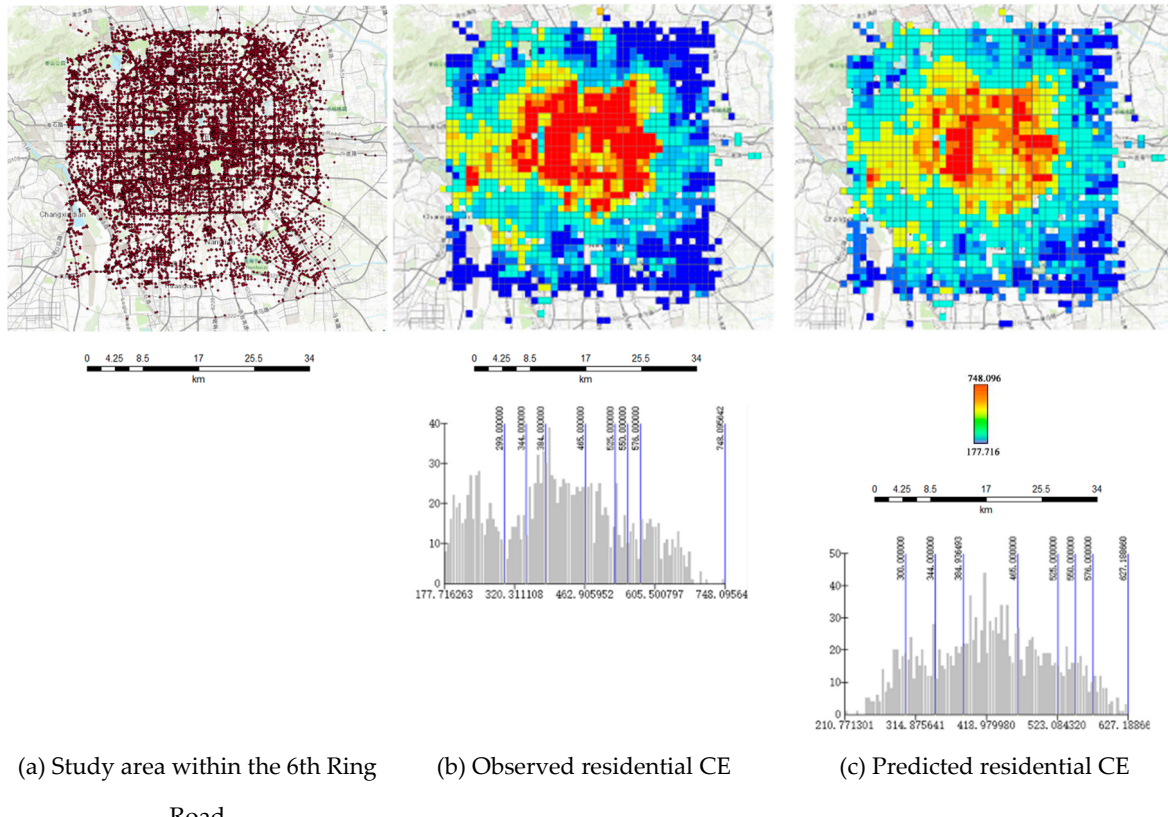
scaled UFP (ultrafine particle) concentrations have a close connection with the surface turbulence and built environment of buildings in urban areas. And CE are also in the form of particles in the air and are related to the constructions in the streets.

Natural features such as trees and grass are reversely related to residential CE since plants can absorb carbon dioxide through photosynthesis, thus reducing the carbon content concentration in the street. In streets near parks and other green areas, where the microclimate is adjusted by trees and other natural elements, the carbon concentration is relatively low.

#### 4.4. Model Visualization and Model Application Scenarios

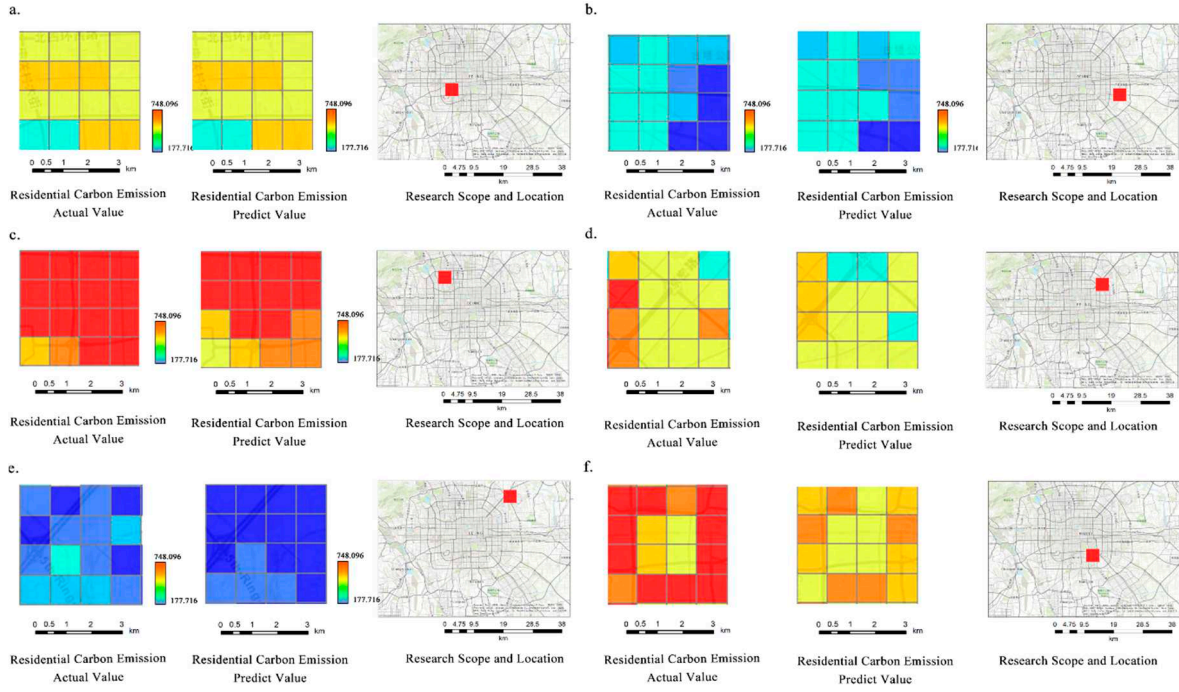
To better visualize the CE predication results, ArcGIS was used to illustrate the difference between actual and predicted residential CE values within each 1KM urban grid (Figure 9). The actual CE value ranges between 177-748 t/km<sup>2</sup>/month, therefore the estimated CE is also visualized in the same scale, to be more immediate comparable.

Figure 10 clearly depicts a relatively reliable prediction of CE values, as overall there are not distinct divergences between the predicted and actual CE values. However, certain deviations were observed across the Beijing urban area. Notably, a significant portion of the city registered lower predicted CE than the actual recorded values. Interestingly, this trend shifts at the urban fringes, where our model consistently predicts higher emissions than what's been observed. This variance could be indicative of underlying complexities in the urban-peripheral dynamics that may not be fully encapsulated by the current model. These findings are invaluable, highlighting potential areas of refinement in our predictive mechanisms, especially concerning the nuanced interplay at the city's outskirts. Figure 9 indicates that prediction accuracy is higher when the ground truth value falls in a certain range (350-550 t/km<sup>2</sup>/month). When the actual CE are low and high, the accuracy of the predicted values will be low. The range of actual CE is 177.72-748.10 t/km<sup>2</sup>/month, while the predicted range is 210.77-627.19 t/km<sup>2</sup>/month.



**Figure 9.** Comparison between Actual and Predicted CE Value Model.

Given the spatial heterogeneity of prediction residual, we selected six areas of 16-square-kilometer urban areas to investigate the divergence between the actual and predicted data. These six areas are distributed in various parts of Beijing (Figure 10). Among them, the MAEs in Figure 10a,b,d are smaller, indicating better prediction accuracy. It can be seen from the comparison of Figure 10c,e that there exist quite great gaps in the prediction of extremely high value and extremely low value, and the accuracy performs not that good. In Figure 10f, which is similar to the average level, but there is still a certain gap when predicting higher CE values.



**Figure 10.** Comparison between Actual and Predicted CE Value Model by MAE in  $t/km^2/month$ : (a) MAE 21.10, (b) MAE 34.33, (c) MAE 57.95, (e) MAE 33.71, (f) MAE 65.33, (d) MAE 40.96.

To the best of our knowledge, currently there are just few mesoscale residential CE models (Jiang et al., 2022). As a cross-reference validation, we selected three similar studies that also focus on household residential and travel CE to compare with our CE model. Compared with these prior studies, our model achieves a similar level accuracy with simply one publicly available input variable, while others normally use more than five types of data inputs (Table 4).

That said, this study not only proposed a model that can better predict residents' carbon emissions on a small scale. More importantly, we verified the possibility of using street view, a simple data source, to predict residents' carbon emissions, supporting simpler data sources for a wide geographical region. A more timely and finer-grained carbon emission prediction model can be potentially established for cities where data availability is limited, especially those in the developing countries.

**Table 4.** Summary of Literature in CE Prediction.

Literature	Dep. Variable	Independent Var.		Model Performance			
		NO. of Data Sources	Type of Variables	S.D.	MAE	RMSE	R <sup>2</sup>
Jiang <i>et al.</i> , 2022	Household travel CE in Guangzhou (kg/week)	5	Socio-economic, household, land use, street forms, location	5.7	12.7	N/A	0.418 (pseudo R <sup>2</sup> )
Zhang, Xiong and Song, 2022	China's annual CE (mt/year)	6	Forest coverage, total energy consumption, energy consumption intensity, GDP, industrial structure, employment structure	2850.1	405.5	525.2	N/A
Zhou, Zhang and Hu, 2021	CE in China	6	Renewable energy development, market demand changes, energy industry regulations, industrial structure reforms, industrial technology innovation, and accidental events.	N/A	N/A	N/A	0.74-0.77
This paper	Residential CE (t/km <sup>2</sup> /month)	1	SVIs	131.12	40.9	58.11	0.8

## 5. Conclusions and Limitations

### 5.1. Effects of Micro-Level Streetscape Attributes

Our SVI based prediction model is a novel tool to predict the residential CE in meso-scale urban area according to the street view images publicly available (i.e., Google/Baidu map). The model can follow the temporal and spatial changes well to predict. Because our model can be used for data visualization and data prediction, it can provide effective CE data for policy makers and urban planners in public environmental protection. The model reflects the influences of specific features on residential CE, so it could provide urban designers with simulation experiments on specific environmental influencing factors. For researchers, our approach presents a new perspective for predicting data and increases the application of machine learning in multi-disciplines. In addition, the visual expression of the model also provides the possibility for ordinary citizens to participate in public decision-making and living place choosing.

This study makes the following contributions. First, compared to other elements of street view, elements like sidewalk, road, fence, building facade and wall are highly relative with the residential CE. Second, using one data of a district in Beijing can measure relatively precisely another district's residential CE in Beijing. The training results from this mode could be used not only to suburban areas but also to urban areas, with the development potential of universality and generalization. The transferability of the model can provide reference for more research on regional CE in the long term. Third, study on the connection between CE and streetscape elements can be conducive to the creation of urban environment under the concept of low-carbon design. Let the goals of sustainable development and carbon neutrality have a foothold to be promoted and optimized on a large scale.

### 5.2. Limitations

In the previous discussion, we compared the different SVIs features and the differences in CE of the specific areas in Chaoyang, including the prosperous areas with high population density, CBD areas, suburbs, industrial areas, etc. to discuss the model's transferability in different urban scenarios.

Although the experimental area selected in this study is the one that has the most rich and diverse urban forms in Beijing, the model's transferability in different cities remains to be verified, especially for those whose energy consumption composition and residents' living habits are very different from those of Beijing. In addition, the model of this study is affected by the features and uncertainties of the input data in the estimation of residential CE. In the process of training and data screening, the quality and representativeness of the data will directly affect the model performance. In this study, through screening and comparison, 22 variables of street features were finally adopted, but these variables do not necessarily represent all relevant variables at the street level. In the meanwhile, the street scenes we study mainly focus on urban arterial roads. There is a lack of certain data for pedestrian blocks. For pedestrian blocks or commercial blocks blocked by other elements (such as canopies, billboards, etc.), there may be certain errors. In addition, since the residential CE data grid is 1km, the CE corresponding to the street observation points in the same grid are of the same value, so the obtained residential CE value cannot fully represent the location of CE. Ideally, each street observation point should have a corresponding accurate residential CE value.

## Reference

Ahmad, T. *et al.* (2018) 'A comprehensive overview on the data driven and large scale based approaches for forecasting of building energy demand: A review', *Energy and Buildings*, 165, pp. 301–320. Available at: <https://doi.org/10.1016/j.enbuild.2018.01.017>.

Baiocchi, G., Minx, J. and Hubacek, K. (2010) 'The Impact of Social Factors and Consumer Behavior on Carbon Dioxide Emissions in the United Kingdom', *Journal of Industrial Ecology*, 14(1), pp. 50–72. Available at: <https://doi.org/10.1111/j.1530-9290.2009.00216.x>.

Berkhout, F., Hertin, J. and Jordan, A. (2002) 'Socio-economic futures in climate change impact assessment: using scenarios as "learning machines"', *Global Environmental Change*, 12(2), pp. 83–95. Available at: [https://doi.org/10.1016/S0959-3780\(02\)00006-7](https://doi.org/10.1016/S0959-3780(02)00006-7).

Birge, D. *et al.* (2019) 'Potential for sustainable use of trees in hot arid regions: A case study of Emirati neighborhoods in Abu Dhabi', *Landscape and Urban Planning*, 190, p. 103577. Available at: <https://doi.org/10.1016/j.landurbplan.2019.05.008>.

Boehme, P., Berger, M. and Massier, T. (2015) 'Estimating the building based energy consumption as an anthropogenic contribution to urban heat islands', *Sustainable Cities and Society*, 19, pp. 373–384. Available at: <https://doi.org/10.1016/j.scs.2015.05.006>.

Bolón-Canedo, V. and Remeseiro, B. (2020) 'Feature selection in image analysis: a survey', *Artificial Intelligence Review*, 53(4), pp. 2905–2931. Available at: <https://doi.org/10.1007/s10462-019-09750-3>.

Cai, M. *et al.* (2021) 'The need for urban form data in spatial modeling of urban carbon emissions in China: A critical review', *Journal of Cleaner Production*, 319, p. 128792. Available at: <https://doi.org/10.1016/j.jclepro.2021.128792>.

Cao, M. *et al.* (2020) 'Estimating Chinese rural and urban residents' carbon consumption and its drivers: considering capital formation as a productive input', *Environment, Development and Sustainability*, 22(6), pp. 5443–5464. Available at: <https://doi.org/10.1007/s10668-019-00432-2>.

Cao, S. *et al.* (2022) 'Effects and contributions of meteorological drought on agricultural drought under different climatic zones and vegetation types in Northwest China', *Science of The Total Environment*, 821, p. 153270. Available at: <https://doi.org/10.1016/j.scitotenv.2022.153270>.

Carrasco-Hernandez, R., Smedley, A.R.D. and Webb, A.R. (2015) 'Using urban canyon geometries obtained from Google Street View for atmospheric studies: Potential applications in the calculation of street level total shortwave irradiances', *Energy and Buildings*, 86, pp. 340–348. Available at: <https://doi.org/10.1016/j.enbuild.2014.10.001>.

Cheng, J. *et al.* (2022) 'Implementation strategies for sustainable renewal at the neighborhood level with the goal of reducing carbon emission', *Sustainable Cities and Society*, 85, p. 104047. Available at: <https://doi.org/10.1016/j.scs.2022.104047>.

Choi, W. *et al.* (2016) 'The effects of the built environment, traffic patterns, and micrometeorology on street level ultrafine particle concentrations at a block scale: Results from multiple urban sites', *Science of The Total Environment*, 553, pp. 474–485. Available at: <https://doi.org/10.1016/j.scitotenv.2016.02.083>.

Christen, A. (2014) 'Atmospheric measurement techniques to quantify greenhouse gas emissions from cities', *Urban Climate*, 10, pp. 241–260. Available at: <https://doi.org/10.1016/j.uclim.2014.04.006>.

Chuai, X. and Feng, J. (2019) 'High resolution carbon emissions simulation and spatial heterogeneity analysis based on big data in Nanjing City, China', *Science of The Total Environment*, 686, pp. 828–837. Available at: <https://doi.org/10.1016/j.scitotenv.2019.05.138>.

Crisp, D. (2010) 'Measuring CO<sub>2</sub> from Space: The NASA Orbiting Carbon Observatory-2', in. *International Astronautical Congress*, Prague. Available at: <https://ntrs.nasa.gov/citations/20150008940> (Accessed: 28 January 2024).

CSC (2021) *The Fourteenth Five-Year Plan*. China's State Council. Available at: [http://www.gov.cn/xinwen/2021-03/13/content\\_5592681.htm](http://www.gov.cn/xinwen/2021-03/13/content_5592681.htm).

Dong, L. *et al.* (2023) 'Assessing impacts of objective features and subjective perceptions of street environment on running amount: A case study of Boston', *Landscape and Urban Planning*, 235, p. 104756. Available at: <https://doi.org/10.1016/j.landurbplan.2023.104756>.

Druckman, A. and Jackson, T. (2008) 'Household energy consumption in the UK: A highly geographically and socio-economically disaggregated model', *Energy Policy*, 36(8), pp. 3177–3192. Available at: <https://doi.org/10.1016/j.enpol.2008.03.021>.

Du, K. and Li, J. (2019) 'Towards a green world: How do green technology innovations affect total-factor carbon productivity', *Energy Policy*, 131, pp. 240–250. Available at: <https://doi.org/10.1016/j.enpol.2019.04.033>.

Du, L. *et al.* (2018) 'System dynamic modeling of urban carbon emissions based on the regional National Economy and Social Development Plan: A case study of Shanghai city', *Journal of Cleaner Production*, 172, pp. 1501–1513. Available at: <https://doi.org/10.1016/j.jclepro.2017.10.128>.

Du, R., Liu, C.-H. and Li, X.-X. (2024) 'A new method for detecting urban morphology effects on urban-scale air temperature and building energy consumption under mesoscale meteorological conditions', *Urban Climate*, 53, p. 101775. Available at: <https://doi.org/10.1016/j.uclim.2023.101775>.

Dubey, A. *et al.* (2016) 'Deep Learning the City: Quantifying Urban Perception at a Global Scale', in B. Leibe *et al.* (eds) *Computer Vision – ECCV 2016*. Cham: Springer International Publishing (Lecture Notes in Computer Science), pp. 196–212. Available at: [https://doi.org/10.1007/978-3-319-46448-0\\_12](https://doi.org/10.1007/978-3-319-46448-0_12).

Dwyer, J.F. *et al.* (2000) *Connecting people with ecosystems in the 21st century: an assessment of our nation's urban forests*. PNW-GTR-490. Portland, OR: U.S. Department of Agriculture, Forest Service, Pacific Northwest Research Station, p. PNW-GTR-490. Available at: <https://doi.org/10.2737/PNW-GTR-490>.

Ehsani, M., Ahmadi, A. and Fadai, D. (2016) 'Modeling of vehicle fuel consumption and carbon dioxide emission in road transport', *Renewable and Sustainable Energy Reviews*, 53, pp. 1638–1648. Available at: <https://doi.org/10.1016/j.rser.2015.08.062>.

Fan, J.-L. *et al.* (2013) 'Residential carbon emission evolutions in urban–rural divided China: An end-use and behavior analysis', *Applied Energy*, 101, pp. 323–332. Available at: <https://doi.org/10.1016/j.apenergy.2012.01.020>.

Fang, C., Wang, S. and Li, G. (2015) 'Changing urban forms and carbon dioxide emissions in China: A case study of 30 provincial capital cities', *Applied Energy*, 158, pp. 519–531. Available at: <https://doi.org/10.1016/j.apenergy.2015.08.095>.

Fang, F. *et al.* (2022) 'Spatial context-aware method for urban land use classification using street view images', *ISPRS Journal of Photogrammetry and Remote Sensing*, 192, pp. 1–12. Available at: <https://doi.org/10.1016/j.isprsjprs.2022.07.020>.

Feng, L. *et al.* (2016) 'Estimates of European uptake of CO<sub>2</sub> inferred from GOSAT X<sub>CO<sub>2</sub></sub> retrievals: sensitivity to measurement bias inside and outside Europe', *Atmospheric Chemistry and Physics*, 16(3), pp. 1289–1302. Available at: <https://doi.org/10.5194/acp-16-1289-2016>.

Frankenberg, C. and Berry, J. (2018) '3.10 - Solar Induced Chlorophyll Fluorescence: Origins, Relation to Photosynthesis and Retrieval', in S. Liang (ed.) *Comprehensive Remote Sensing*. Oxford: Elsevier, pp. 143–162. Available at: <https://doi.org/10.1016/B978-0-12-409548-9.10632-3>.

Gao, S., Janowicz, K. and Couclelis, H. (2017) 'Extracting urban functional regions from points of interest and human activities on location-based social networks', *Transactions in GIS*, 21(3), pp. 446–467. Available at: <https://doi.org/10.1111/tgis.12289>.

Gately, C.K. and Hutyra, L.R. (2017) 'Large Uncertainties in Urban-Scale Carbon Emissions', *Journal of Geophysical Research: Atmospheres*, 122(20), p. 11,242-11,260. Available at: <https://doi.org/10.1002/2017JD027359>.

Gong, F.-Y. *et al.* (2018) 'Mapping sky, tree, and building view factors of street canyons in a high-density urban environment', *Building and Environment*, 134, pp. 155–167. Available at: <https://doi.org/10.1016/j.buildenv.2018.02.042>.

Gregg, J.S. and Andres, R.J. (2008) 'A method for estimating the temporal and spatial patterns of carbon dioxide emissions from national fossil-fuel consumption', *Tellus B: Chemical and Physical Meteorology*, 60(1), pp. 1–10. Available at: <https://doi.org/10.1111/j.1600-0889.2007.00319.x>.

Griew, P. *et al.* (2013) 'Developing and testing a street audit tool using Google Street View to measure environmental supportiveness for physical activity', *International Journal of Behavioral Nutrition and Physical Activity*, 10(1), p. 103. Available at: <https://doi.org/10.1186/1479-5868-10-103>.

Guo, Y. *et al.* (2018) 'A review of semantic segmentation using deep neural networks', *International Journal of Multimedia Information Retrieval*, 7(2), pp. 87–93. Available at: <https://doi.org/10.1007/s13735-017-0141-z>.

Gurney, K.R. *et al.* (2012) 'Quantification of Fossil Fuel CO<sub>2</sub> Emissions on the Building/Street Scale for a Large U.S. City', *Environmental Science & Technology*, 46(21), pp. 12194–12202. Available at: <https://doi.org/10.1021/es301128z>.

Gurney, K.R. *et al.* (2019) 'Comparison of Global Downscaled Versus Bottom-Up Fossil Fuel CO<sub>2</sub> Emissions at the Urban Scale in Four U.S. Urban Areas', *Journal of Geophysical Research: Atmospheres*, 124(5), pp. 2823–2840. Available at: <https://doi.org/10.1029/2018JD028859>.

Ha, J. *et al.* (2023) 'Mode choice and the first-/last-mile burden: The moderating effect of street-level walkability', *Transportation Research Part D: Transport and Environment*, 116, p. 103646. Available at: <https://doi.org/10.1016/j.trd.2023.103646>.

Hakkarainen, J., Ialongo, I. and Tamminen, J. (2016) 'Direct space-based observations of anthropogenic CO<sub>2</sub> emission areas from OCO-2', *Geophysical Research Letters*, 43(21), p. 11,400-11,406. Available at: <https://doi.org/10.1002/2016GL070885>.

He, W., Liu, D. and Wang, C. (2022) 'Are Chinese provincial carbon emissions allowances misallocated over 2000–2017? Evidence from an extended Gini-coefficient approach', *Sustainable Production and Consumption*, 29, pp. 564–573. Available at: <https://doi.org/10.1016/j.spc.2021.11.007>.

Helm, J.M. *et al.* (2020) 'Machine Learning and Artificial Intelligence: Definitions, Applications, and Future Directions', *Current Reviews in Musculoskeletal Medicine*, 13(1), pp. 69–76. Available at: <https://doi.org/10.1007/s12178-020-09600-8>.

Hong, X. *et al.* (2022) 'Retrieval of Global Carbon Dioxide From TanSat Satellite and Comprehensive Validation With TCCON Measurements and Satellite Observations', *IEEE Transactions on Geoscience and Remote Sensing*, 60, pp. 1–16. Available at: <https://doi.org/10.1109/TGRS.2021.3066623>.

Huang, C. and Tao, J. (2020) 'Chapter 4 - Water-related problems with special reference to global climate change in China', in P. Singh *et al.* (eds) *Water Conservation and Wastewater Treatment in BRICS Nations*. Elsevier, pp. 61–82. Available at: <https://doi.org/10.1016/B978-0-12-818339-7.00004-7>.

Huang, W. *et al.* (2022) 'Estimating urban functional distributions with semantics preserved POI embedding', *International Journal of Geographical Information Science*, 36(10), pp. 1905–1930. Available at: <https://doi.org/10.1080/13658816.2022.2040510>.

Ignatius, M. *et al.* (2022) 'LOCAL CLIMATE ZONES: LESSONS FROM SINGAPORE AND POTENTIAL IMPROVEMENT WITH STREET VIEW IMAGERY', *ISPRS Annals of the Photogrammetry, Remote Sensing and Spatial Information Sciences*, X-4-W2-2022, pp. 121–128. Available at: <https://doi.org/10.5194/isprs-annals-X-4-W2-2022-121-2022>.

Ito, K. and Biljecki, F. (2021) 'Assessing bikeability with street view imagery and computer vision', *Transportation Research Part C: Emerging Technologies*, 132, p. 103371. Available at: <https://doi.org/10.1016/j.trc.2021.103371>.

Jain, A.K., Meiyappan, P. and Richardson, T. (2013) 'Carbon Emissions from Land-Use Change: Model Estimates Using Three Different Data Sets', in B.C. Reed *et al.* (eds) *Land Use and the Carbon Cycle: Advances in Integrated Science, Management, and Policy*. Cambridge: Cambridge University Press, pp. 241–258. Available at: <https://doi.org/10.1017/CBO9780511894824.013>.

Jiang, L. *et al.* (2022) 'Household Energy Consumption Patterns and Carbon Emissions for the Megacities—Evidence from Guangzhou, China', *Energies*, 15(8), p. 2731. Available at: <https://doi.org/10.3390/en15082731>.

Jiang, Y. *et al.* (2019) 'Modelling household travel energy consumption and CO<sub>2</sub> emissions based on the spatial form of neighborhoods and streets: A case study of Jinan, China', *Computers, Environment and Urban Systems*, 77, p. 101134. Available at: <https://doi.org/10.1016/j.compenvurbsys.2017.03.005>.

Jiang, Y., Jiang, S. and Shi, T. (2020) 'Comparative Study on the Cooling Effects of Green Space Patterns in Waterfront Build-Up Blocks: An Experience from Shanghai', *International Journal of Environmental Research and Public Health*, 17(22), p. 8684. Available at: <https://doi.org/10.3390/ijerph17228684>.

Joint Research Centre (European Commission) *et al.* (2023) *GHG emissions of all world countries: 2023*. LU: Publications Office of the European Union. Available at: <https://data.europa.eu/doi/10.2760/953322> (Accessed: 23 January 2024).

Jordan, M.I. and Mitchell, T.M. (2015) 'Machine learning: Trends, perspectives, and prospects', *Science*, 349(6245), pp. 255–260. Available at: <https://doi.org/10.1126/science.aaa8415>.

Kabir, H. and Garg, N. (2023) 'Machine learning enabled orthogonal camera goniometry for accurate and robust contact angle measurements', *Scientific Reports*, 13(1), p. 1497. Available at: <https://doi.org/10.1038/s41598-023-28763-1>.

Kaya, Y. (1989) 'Impact of carbon dioxide emission control on GNP growth: Interpretation of proposed scenarios', *Intergovernmental Panel on Climate Change/Response Strategies Working Group, May* [Preprint]. Available at: <https://cir.nii.ac.jp/crid/1570291225678384256> (Accessed: 29 January 2024).

Kelly, C.M. *et al.* (2013) 'Using Google Street View to Audit the Built Environment: Inter-rater Reliability Results', *Annals of Behavioral Medicine*, 45(suppl\_1), pp. S108–S112. Available at: <https://doi.org/10.1007/s12160-012-9419-9>.

Koo, B.W. *et al.* (2023) 'Can good microscale pedestrian streetscapes enhance the benefits of macroscale accessible urban form? An automated audit approach using Google street view images', *Landscape and Urban Planning*, 237, p. 104816. Available at: <https://doi.org/10.1016/j.landurbplan.2023.104816>.

Kumar, A. *et al.* (2023) 'Greenhouse gas emissions from hydroelectric reservoirs: mechanistic understanding of influencing factors and future prospect', *Environmental Science and Pollution Research* [Preprint]. Available at: <https://doi.org/10.1007/s11356-023-25717-y>.

Li, W. and Joh, K. (2017) 'Exploring the synergistic economic benefit of enhancing neighbourhood bikeability and public transit accessibility based on real estate sale transactions', *Urban Studies*, 54(15), pp. 3480–3499. Available at: <https://doi.org/10.1177/0042098016680147>.

Li, Z. *et al.* (2022) 'Exploring differentiated impacts of socioeconomic factors and urban forms on city-level CO<sub>2</sub> emissions in China: Spatial heterogeneity and varying importance levels', *Sustainable Cities and Society*, 84, p. 104028. Available at: <https://doi.org/10.1016/j.scs.2022.104028>.

Liang, X., Zhao, T. and Biljecki, F. (2023) 'Revealing spatio-temporal evolution of urban visual environments with street view imagery', *Landscape and Urban Planning*, 237, p. 104802. Available at: <https://doi.org/10.1016/j.landurbplan.2023.104802>.

Liu, J., Li, S. and Ji, Q. (2021) 'Regional differences and driving factors analysis of carbon emission intensity from transport sector in China', *Energy*, 224, p. 120178. Available at: <https://doi.org/10.1016/j.energy.2021.120178>.

Liu, X. *et al.* (2019) 'Scenario simulation of urban energy-related CO<sub>2</sub> emissions by coupling the socioeconomic factors and spatial structures', *Applied Energy*, 238, pp. 1163–1178. Available at: <https://doi.org/10.1016/j.apenergy.2019.01.173>.

Lu, Y. *et al.* (2023) 'Assessing urban greenery by harvesting street view data: A review', *Urban Forestry & Urban Greening*, 83, p. 127917. Available at: <https://doi.org/10.1016/j.ufug.2023.127917>.

Malakouti, S.M. (2023) 'Babysitting hyperparameter optimization and 10-fold-cross-validation to enhance the performance of ML methods in predicting wind speed and energy generation', *Intelligent Systems with Applications*, 19, p. 200248. Available at: <https://doi.org/10.1016/j.iswa.2023.200248>.

Middel, A. *et al.* (2019) 'Urban form and composition of street canyons: A human-centric big data and deep learning approach', *Landscape and Urban Planning*, 183, pp. 122–132. Available at: <https://doi.org/10.1016/j.landurbplan.2018.12.001>.

Nowak, D.J. and Crane, D.E. (2002) 'Carbon storage and sequestration by urban trees in the USA', *Environmental Pollution*, 116(3), pp. 381–389. Available at: [https://doi.org/10.1016/S0269-7491\(01\)00214-7](https://doi.org/10.1016/S0269-7491(01)00214-7).

Ogle, S.M. *et al.* (2015) 'An approach for verifying biogenic greenhouse gas emissions inventories with atmospheric CO<sub>2</sub> concentration data', *Environmental Research Letters*, 10(3), p. 034012. Available at: <https://doi.org/10.1088/1748-9326/10/3/034012>.

Ou, J. *et al.* (2013) 'Quantifying the relationship between urban forms and carbon emissions using panel data analysis', *Landscape Ecology*, 28(10), pp. 1889–1907. Available at: <https://doi.org/10.1007/s10980-013-9943-4>.

Ou, J. *et al.* (2019) 'Investigating the differentiated impacts of socioeconomic factors and urban forms on CO<sub>2</sub> emissions: Empirical evidence from Chinese cities of different developmental levels', *Journal of Cleaner Production*, 226, pp. 601–614. Available at: <https://doi.org/10.1016/j.jclepro.2019.04.123>.

Pachauri, S. (2004) 'An analysis of cross-sectional variations in total household energy requirements in India using micro survey data', *Energy Policy*, 32(15), pp. 1723–1735. Available at: [https://doi.org/10.1016/S0301-4215\(03\)00162-9](https://doi.org/10.1016/S0301-4215(03)00162-9).

Pao, H.-T. and Tsai, C.-M. (2011) 'Modeling and forecasting the CO<sub>2</sub> emissions, energy consumption, and economic growth in Brazil', *Energy*, 36(5), pp. 2450–2458. Available at: <https://doi.org/10.1016/j.energy.2011.01.032>.

Park, H.-C. and Heo, E. (2007) 'The direct and indirect household energy requirements in the Republic of Korea from 1980 to 2000—An input–output analysis', *Energy Policy*, 35(5), pp. 2839–2851. Available at: <https://doi.org/10.1016/j.enpol.2006.10.002>.

Peng, C. (2016) 'Calculation of a building's life cycle carbon emissions based on Ecotect and building information modeling', *Journal of Cleaner Production*, 112, pp. 453–465. Available at: <https://doi.org/10.1016/j.jclepro.2015.08.078>.

Qian, L. *et al.* (2022) 'Carbon emission reduction effects of eco-industrial park policy in China', *Energy*, 261, p. 125315. Available at: <https://doi.org/10.1016/j.energy.2022.125315>.

Qiu, W. *et al.* (2021) 'Subjectively Measured Streetscape Perceptions to Inform Urban Design Strategies for Shanghai', *ISPRS International Journal of Geo-Information*, 10(8), p. 493. Available at: <https://doi.org/10.3390/ijgi10080493>.

Qiu, W. *et al.* (2022) 'Subjective or objective measures of street environment, which are more effective in explaining housing prices?', *Landscape and Urban Planning*, 221, p. 104358. Available at: <https://doi.org/10.1016/j.landurbplan.2022.104358>.

Qiu, W. *et al.* (2023) 'Subjective and objective measures of streetscape perceptions: Relationships with property value in Shanghai', *Cities*, 132, p. 104037. Available at: <https://doi.org/10.1016/j.cities.2022.104037>.

Qiu, W. and Chang, H. (2021) 'The interplay between dockless bikeshare and bus for small-size cities in the US: A case study of Ithaca', *Journal of Transport Geography*, 96, p. 103175. Available at: <https://doi.org/10.1016/j.jtrangeo.2021.103175>.

Quan, S.J. et al. (2016) 'Urban Form and Building Energy Performance in Shanghai Neighborhoods', *Energy Procedia*, 88, pp. 126–132. Available at: <https://doi.org/10.1016/j.egypro.2016.06.035>.

Queralt, A. et al. (2021) 'Reliability of streetscape audits comparing on-street and online observations: MAPS-Global in 5 countries', *International Journal of Health Geographics*, 20(1), p. 6. Available at: <https://doi.org/10.1186/s12942-021-00261-5>.

Resch, E. et al. (2016) 'Impact of Urban Density and Building Height on Energy Use in Cities', *Energy Procedia*, 96, pp. 800–814. Available at: <https://doi.org/10.1016/j.egypro.2016.09.142>.

Ribeiro, H.V., Rybski, D. and Kropp, J.P. (2019) 'Effects of changing population or density on urban carbon dioxide emissions', *Nature Communications*, 10(1), p. 3204. Available at: <https://doi.org/10.1038/s41467-019-11184-y>.

Rundle, A.G. et al. (2011) 'Using Google Street View to Audit Neighborhood Environments', *American Journal of Preventive Medicine*, 40(1), pp. 94–100. Available at: <https://doi.org/10.1016/j.amepre.2010.09.034>.

Ryu, H. et al. (2014) 'Electricity-generation mix considering energy security and carbon emission mitigation: Case of Korea and Mongolia', *Energy*, 64, pp. 1071–1079. Available at: <https://doi.org/10.1016/j.energy.2013.10.089>.

Salesses, P., Schechtner, K. and Hidalgo, C.A. (2013) 'The Collaborative Image of The City: Mapping the Inequality of Urban Perception', *PLOS ONE*, 8(7), p. e68400. Available at: <https://doi.org/10.1371/journal.pone.0068400>.

Sallis, J.F. et al. (2006) 'An ecological approach to creating active living communities', *Annual Review of Public Health*, 27, pp. 297–322. Available at: <https://doi.org/10.1146/annurev.publhealth.27.021405.102100>.

Schuh, A.E. et al. (2013) 'Evaluating atmospheric CO<sub>2</sub> inversions at multiple scales over a highly inventoried agricultural landscape', *Global Change Biology*, 19(5), pp. 1424–1439. Available at: <https://doi.org/10.1111/gcb.12141>.

Seiferling, I. et al. (2017) 'Green streets – Quantifying and mapping urban trees with street-level imagery and computer vision', *Landscape and Urban Planning*, 165, pp. 93–101. Available at: <https://doi.org/10.1016/j.landurbplan.2017.05.010>.

Shao, L. et al. (2016) 'Carbon emissions from fossil fuel consumption of Beijing in 2012', *Environmental Research Letters*, 11(11), p. 114028. Available at: <https://doi.org/10.1088/1748-9326/11/11/114028>.

Shen, Y.-S. et al. (2022) 'Crucial factors of the built environment for mitigating carbon emissions', *Science of The Total Environment*, 806, p. 150864. Available at: <https://doi.org/10.1016/j.scitotenv.2021.150864>.

Shi, C. et al. (2022) 'How carbon emission reduction is going to affect urban resilience', *Journal of Cleaner Production*, 372, p. 133737. Available at: <https://doi.org/10.1016/j.jclepro.2022.133737>.

Shi, K. et al. (2020) 'Effects of urban forms on CO<sub>2</sub> emissions in China from a multi-perspective analysis', *Journal of Environmental Management*, 262, p. 110300. Available at: <https://doi.org/10.1016/j.jenvman.2020.110300>.

Shu, X. et al. (2018) 'Relationships between carbon emission, urban growth, and urban forms of urban agglomeration in the Yangtze River Delta', *Ecological Indicators*, 38(17), pp. 6302–6313. Available at: <https://doi.org/10.5846/stxb201707101242>.

Song, Q. et al. (2022) 'Investigating the Impact of Perceived Micro-Level Neighborhood Characteristics on Housing Prices in Shanghai', *Land*, 11(11), p. 2002. Available at: <https://doi.org/10.3390/land1112002>.

Song, Q. et al. (2023) 'Disclosing the Impact of Micro-level Environmental Characteristics on Dockless Bikeshare Trip Volume: A Case Study of Ithaca', in R. Goodspeed et al. (eds) *Intelligence for Future Cities*. Cham: Springer Nature Switzerland (The Urban Book Series), pp. 125–147. Available at: [https://doi.org/10.1007/978-3-031-31746-0\\_8](https://doi.org/10.1007/978-3-031-31746-0_8).

Song, Y. et al. (2021) 'Assessing block-level sustainable transport infrastructure development using a spatial trade-off relation model', *International Journal of Applied Earth Observation and Geoinformation*, 105, p. 102585. Available at: <https://doi.org/10.1016/j.jag.2021.102585>.

Steinmetz-Wood, M. et al. (2019) 'Assessing the micro-scale environment using Google Street View: the Virtual Systematic Tool for Evaluating Pedestrian Streetscapes (Virtual-STEPS)', *BMC Public Health*, 19(1), p. 1246. Available at: <https://doi.org/10.1186/s12889-019-7460-3>.

Stewart, I. and Oke, T. (2009) 'CLASSIFYING URBAN CLIMATE FIELD SITES BY "LOCAL CLIMATE ZONES": THE CASE OF NAGANO, JAPAN'.

Stewart, I.D. and Oke, T.R. (2012) 'Local Climate Zones for Urban Temperature Studies', *Bulletin of the American Meteorological Society*, 93(12), pp. 1879–1900. Available at: <https://doi.org/10.1175/BAMS-D-11-00019.1>.

Su, N., Li, W. and Qiu, W. (2023) 'Measuring the associations between eye-level urban design quality and on-street crime density around New York subway entrances', *Habitat International*, 131, p. 102728. Available at: <https://doi.org/10.1016/j.habitatint.2022.102728>.

Su, S. *et al.* (2022) 'Deciphering the influence of TOD on metro ridership: An integrated approach of extended node-place model and interpretable machine learning with planning implications', *Journal of Transport Geography*, 104, p. 103455. Available at: <https://doi.org/10.1016/j.jtrangeo.2022.103455>.

Sun, D. (Jian) *et al.* (2017) 'Modeling carbon emissions from urban traffic system using mobile monitoring', *Science of The Total Environment*, 599–600, pp. 944–951. Available at: <https://doi.org/10.1016/j.scitotenv.2017.04.186>.

Sun, H. *et al.* (2023) 'A Spatial Analysis of Urban Streets under Deep Learning Based on Street View Imagery: Quantifying Perceptual and Elemental Perceptual Relationships', *Sustainability*, 15(20), p. 14798. Available at: <https://doi.org/10.3390/su152014798>.

Thompson, D.R. *et al.* (2016) 'Space-based remote imaging spectroscopy of the Aliso Canyon CH<sub>4</sub> superemitter', *Geophysical Research Letters*, 43(12), pp. 6571–6578. Available at: <https://doi.org/10.1002/2016GL069079>.

Tian, H., Han, Z. and Xu, W. (2021) *Evolution of Historical Urban Landscape with Computer Vision and Machine Learning: A Case Study of Berlin*. DE: Wichmann Verlag. Available at: <https://doi.org/10.14627/537705039> (Accessed: 2 February 2024).

Tranchard, S. (2017) *Measuring the carbon footprint of buildings in a simple way*, ISO. Available at: <https://www.iso.org/cms/render/live/en/sites/isoorg/contents/news/2017/07/Ref2205.html> (Accessed: 26 January 2024).

Vaccari, F.P. *et al.* (2013) 'Carbon dioxide balance assessment of the city of Florence (Italy), and implications for urban planning', *Landscape and Urban Planning*, 120, pp. 138–146. Available at: <https://doi.org/10.1016/j.landurbplan.2013.08.004>.

Wang, J., Liu, W. and Gou, A. (2022) 'Numerical characteristics and spatial distribution of panoramic Street Green View index based on SegNet semantic segmentation in Savannah', *Urban Forestry & Urban Greening*, 69, p. 127488. Available at: <https://doi.org/10.1016/j.ufug.2022.127488>.

Wang, S. *et al.* (2019) 'Estimating the impacts of urban form on CO<sub>2</sub> emission efficiency in the Pearl River Delta, China', *Cities*, 85, pp. 117–129. Available at: <https://doi.org/10.1016/j.cities.2018.08.009>.

Wen, L. and Shao, H. (2019) 'Influencing factors of the carbon dioxide emissions in China's commercial department: A non-parametric additive regression model', *Science of The Total Environment*, 668, pp. 1–12. Available at: <https://doi.org/10.1016/j.scitotenv.2019.02.412>.

Wilson, C. and Dowlatabadi, H. (2007) 'Models of Decision Making and Residential Energy Use', *Annual Review of Environment and Resources*, 32(1), pp. 169–203. Available at: <https://doi.org/10.1146/annurev.energy.32.053006.141137>.

Wu, H., Guo, Z. and Peng, C. (2003) 'Land use induced changes of organic carbon storage in soils of China', *Global Change Biology*, 9(3), pp. 305–315. Available at: <https://doi.org/10.1046/j.1365-2486.2003.00590.x>.

Wu, W., Yao, Y. and Wang, R. (2023) 'Green space exposure at subway stations, transportation mode choice and travel satisfaction', *Transportation Research Part D: Transport and Environment*, 122, p. 103862. Available at: <https://doi.org/10.1016/j.trd.2023.103862>.

Xia, C. *et al.* (2020) 'Spatial-temporal distribution of carbon emissions by daily travel and its response to urban form: A case study of Hangzhou, China', *Journal of Cleaner Production*, 257, p. 120797. Available at: <https://doi.org/10.1016/j.jclepro.2020.120797>.

Xia, Y., Yabuki, N. and Fukuda, T. (2021) 'Sky view factor estimation from street view images based on semantic segmentation', *Urban Climate*, 40, p. 100999. Available at: <https://doi.org/10.1016/j.uclim.2021.100999>.

Xu, C. *et al.* (2022) 'Can improving the spatial equity of urban green space mitigate the effect of urban heat islands? An empirical study', *Science of The Total Environment*, 841, p. 156687. Available at: <https://doi.org/10.1016/j.scitotenv.2022.156687>.

Xu, X., Qiu, W., Li, W., Liu, X., *et al.* (2022) 'Associations between Street-View Perceptions and Housing Prices: Subjective vs. Objective Measures Using Computer Vision and Machine Learning Techniques', *Remote Sensing*, 14(4), p. 891. Available at: <https://doi.org/10.3390/rs14040891>.

Xu, X., Qiu, W., Li, W., Huang, D., *et al.* (2022) 'Comparing satellite image and GIS data classified local climate zones to assess urban heat island: A case study of Guangzhou', *Frontiers in Environmental Science*, 10. Available at: <https://www.frontiersin.org/articles/10.3389/fenvs.2022.1029445> (Accessed: 2 February 2024).

Yan, Y. and Huang, B. (2022) 'Estimation of building height using a single street view image via deep neural networks', *ISPRS Journal of Photogrammetry and Remote Sensing*, 192, pp. 83–98. Available at: <https://doi.org/10.1016/j.isprsjprs.2022.08.006>.

Yoshida, Y. *et al.* (2011) 'Retrieval algorithm for CO<sub>2</sub> and CH<sub>4</sub> column abundances from short-wavelength infrared spectral observations by the Greenhouse gases observing satellite', *Atmospheric Measurement Techniques*, 4(4), pp. 717–734. Available at: <https://doi.org/10.5194/amt-4-717-2011>.

Yu, Y. *et al.* (2022) 'Exploring built environment factors on e-bike travel behavior in urban China: A case study of Jinan', *Frontiers in Public Health*, 10. Available at: <https://www.frontiersin.org/articles/10.3389/fpubh.2022.1013421> (Accessed: 26 January 2024).

Yuan, W., Wang, J. and Xu, W. (2022) 'Shift Pooling PSPNet: Rethinking PSPNet for Building Extraction in Remote Sensing Images from Entire Local Feature Pooling', *Remote Sensing*, 14(19), p. 4889. Available at: <https://doi.org/10.3390/rs14194889>.

Yuan, X., Wang, X. and Zuo, J. (2013) 'Renewable energy in buildings in China—A review', *Renewable and Sustainable Energy Reviews*, 24, pp. 1–8. Available at: <https://doi.org/10.1016/j.rser.2013.03.022>.

Zhang, J. *et al.* (2020) 'Influence of the built environment on urban residential low-carbon cognition in zhengzhou, China', *Journal of Cleaner Production*, 271, p. 122429. Available at: <https://doi.org/10.1016/j.jclepro.2020.122429>.

Zhang, L. *et al.* (2023) 'How road network transformation may be associated with reduced carbon emissions: An exploratory analysis of 19 major Chinese cities', *Sustainable Cities and Society*, 95, p. 104575. Available at: <https://doi.org/10.1016/j.scs.2023.104575>.

Zhang, R., Pu, L. and Zhu, M. (2013) 'Impacts of transportation arteries on land use patterns in urban-rural fringe: A comparative gradient analysis of Qixia District, Nanjing City, China', *Chinese Geographical Science*, 23(3), pp. 378–388. Available at: <https://doi.org/10.1007/s11769-012-0582-5>.

Zhang, T., Song, Y. and Yang, J. (2021) 'Relationships between urbanization and CO2 emissions in China: An empirical analysis of population migration', *PLOS ONE*, 16(8), p. e0256335. Available at: <https://doi.org/10.1371/journal.pone.0256335>.

Zhang, X., Xiong, J. and Song, J. (2022) 'Forecast of China's Annual Carbon Emissions Based on Two-Stage Model', *Frontiers in Environmental Science*, 10. Available at: <https://www.frontiersin.org/articles/10.3389/fenvs.2022.895648> (Accessed: 25 January 2024).

Zhao, H. *et al.* (2017) 'Pyramid Scene Parsing Network', in: *Proceedings of the IEEE Conference on Computer Vision and Pattern Recognition*, pp. 2881–2890. Available at: [https://openaccess.thecvf.com/content\\_cvpr\\_2017/html/Zhao\\_Pyramid\\_Scene\\_Parsing\\_CVPR\\_2017\\_paper\\_r.html](https://openaccess.thecvf.com/content_cvpr_2017/html/Zhao_Pyramid_Scene_Parsing_CVPR_2017_paper_r.html) (Accessed: 23 January 2024).

Zheng, Y. *et al.* (2022) 'Estimating carbon emissions in urban functional zones using multi-source data: A case study in Beijing', *Building and Environment*, 212, p. 108804. Available at: <https://doi.org/10.1016/j.buildenv.2022.108804>.

Zheng, Y. *et al.* (2023) 'Exploring the impact of explicit and implicit urban form on carbon emissions: Evidence from Beijing, China', *Ecological Indicators*, 154, p. 110558. Available at: <https://doi.org/10.1016/j.ecolind.2023.110558>.

Zhou, B. *et al.* (2019) 'Semantic Understanding of Scenes Through the ADE20K Dataset', *International Journal of Computer Vision*, 127(3), pp. 302–321. Available at: <https://doi.org/10.1007/s11263-018-1140-0>.

Zhou, W. *et al.* (2021) 'Forecasting Chinese carbon emissions using a novel grey rolling prediction model', *Chaos, Solitons & Fractals*, 147, p. 110968. Available at: <https://doi.org/10.1016/j.chaos.2021.110968>.

Zhou, Y., Zhang, J. and Hu, S. (2021) 'Regression analysis and driving force model building of CO2 emissions in China', *Scientific Reports*, 11(1), p. 6715. Available at: <https://doi.org/10.1038/s41598-021-86183-5>.

**Disclaimer/Publisher's Note:** The statements, opinions and data contained in all publications are solely those of the individual author(s) and contributor(s) and not of MDPI and/or the editor(s). MDPI and/or the editor(s) disclaim responsibility for any injury to people or property resulting from any ideas, methods, instructions or products referred to in the content.